Monitoring of glaciers and their regional shrinkage over mid-eastern Himalaya using high resolution satellite observations

Sunal OJHA

A dissertation for the degree of Doctor of Environmental Studies

Department of Earth and Environmental Science
Graduate School of Environmental Studies, Nagoya University

Supervisors
Associate professor Koji FUJITA, PhD
Assistant professor Akiko SAKAI, PhD

Nagoya, Japan
January, 2017

Abstract

The Himalayan range scales over 2,400 km in length covering the national territory of Bhutan, India, China and Nepal which feeds the major river basins in Asia. The glaciers in this region are the major source to maintain hydrological regime of the rivers which, in recent decades, receive largest threat to climate change. The scientific evidences show that the glaciers in Himalayan region are retreating at the rate similar to those in other part of the world and more aggressive melting is reported for last few decades.

To enhance our understanding on Himalayan glaciers and to fill the scientific gap between global and regional scale, first we studied 5301 glaciers in mid-eastern Himalaya which covers the area of 5691 ± 893 km^2. Those glaciers were manually delineated by using 104 ALOS derived satellite images. We found that 4459 glaciers covering the area of 1853± 141 km^2 are debris free ice (C-glaciers) whereas 842 glaciers covering the area of 3839 ± 753 km^2 are debris covered (D-glaciers) which is a novel estimation in Mid-eastern Himalaya. Again 842 debris covered glaciers are separated into clean part (C-part) and debris part (D-part) covering the area of 2867 ± 167 km^2 and 971 ± 236 km^2, respectively. This inventory reveals comparatively better status of glaciers as compared to other inventories because of high resolution images (2.4 m, ALOS-PRISM) from recent years were utilized during the delineation. The median elevation of the glaciers in this area is 5605 ± 402 m a.s.l., where D-glaciers (5484 ± 369 m a.s.l.) are clearly situated at lower elevations than C-glaciers (5628 ± 405 m a.s.l.). Similarly, D-glaciers are situated distinctly flatter (27 ± 7º) than that of C-glaciers (31 ± 9º). Over the regional scale, D-part coverage is found to be declining from west (Langtang massif) to east (Bhutan massif). The minimum elevation of glaciers tend to increase from west to east and maximum elevation tend to decrease west to east making elevation range narrower in eastern massifs.

At the second stage, the glacier polygons from ALOS images (2006-2010) are compared with other set of glacier polygon obtained in 1992 based in aerial photographs to analyse decade glaciers shrinkage over the Nepal territory. Our shrinkage analysis is confined to Nepal territory: Ganesh Himal in the west to Kanchenjunga in the east due to limitation on data availability. Since 1992, the total glacier area deceased from 1616 ± 247 km^2 to 1477 ± 232 km^2 giving a − 8.5 % area change (-0.5 ± 0.1 % a^{-1}) during the study period. The area of C-glaciers changes

from 481± 35 km^2 to 427 ± 32 km^2 whereas D-glaciers changes from 1136 ± 212 km^2 to 1050 ± 200 km^2 giving −11.2 % (−0.70 % a^{-1}) and −7.5 % (−0.47 % a^{-1}) area changes, respectively. The small glaciers for both C- and D-type has lost its larger proportion of area whereas medium and large size glaciers has lost its smaller proportion during the last two decades. In total, 61 C-type glaciers covering the area of 2.4 ± 0.3 km^2 has totally disappeared during the study period which is one of the interesting result of this research. The D-glaciers are found to be shrank in lower rate than that of C-glaciers which is due to insulating properties of supraglacial mantle. Our study showed high rate of shrinking in recent decades as compared to similar study done previously in the similar region. Area change shows significant correlations with minimum elevation ($r= 0.30$, $p < 0.0001$), maximum elevation ($r = –0.18$, $p < 0.0001$), altitudinal range ($r = –0.50$, $p < 0.0001$), glacier area ($r = –0.62$, $p < 0.0001$), and mean slope ($r = 0.16$, $p < 0.0001$) suggesting that larger glacier tends to have lost larger area (but smaller percentage) and vice versa. Intra-regional analysis of the glacier change clearly shows high rate of shrinking in western massif as compared to eastern massifs during the study period.

To understand the dynamics of D-part formation, we, thirdly, investigated the relation between D-part area and its corresponding potential debris supply (PDS) slope for 842 D-glaciers. The PDS slopes in southern-side has better correlation with its debris-part formation than that situated in northern-side of Himalayan barrier. The correlation weakens as it goes from eastern to western massifs which can be related to its larger PDS area and steeper PDS slope in western massifs. Further investigation shows PDS slopes facing SE to W orientation has stronger control over D-part formation which is related to diurnal freeze-thaw cycle in southern slope of mountain barrier. The local topography (PDS gradient) also play vital role in dimension of D-part area whereas latitude has less or no influence on D-part formation in this study area.

Key Words: ALOS, Glaciers, Aerial photographs, PDS, Himalayan region.

Table of contents

List of Tables

Lists of Figures

Acronyms and Abbreviation

ALOS	Advanced Land Observing Satellite
ASTER	Advanced Spaceborne Thermal Emission and Reflection
AVNIR-2	Advanced Visible and Near Infrared Radiometer 2
DEM	Digital Elevation Model
DHM	Department of Hydrology and Meteorology
DSM	Digital Surface Model
GLIMS	Global Land Ice Measurements from Space
ICIMOD	International Centre for Integrated Mountain Development
IPCC AR	Intergovernmental Panel on Climate Change Assessment Report
LPS	Leica Photogrammetric Suite
NSIDC	National Snow and Ice Data Center
PDS	Potential Debris Supply
PR	Precipitation radar
PRISM	Panchromatic Remote-sensing Instrument for Stereo Mapping
RPC	Rational Polynomial Coefficient
TM	Thematic Mapper
TRMM	Tropical Rainfall Measuring Mission
UNEP	United Nations Environmental Program
WWF	World Wildlife Fund

1. INTRODUCTION

1.1 Glacier and Climate

Glaciers are the largest reservoir of fresh water spread over the world which amounts roughly 10 percent of earth's land surface totaling the area of 15 million square kilometers (NSIDC, 2016). The glacier around the world is estimated to store 75 percent of world's fresh water. Although glaciers are spread over all continents even in small proportion, the majority of the world glaciers are located in Antarctica, Greenland and Asian mountains which are reported to be contributing to sea level rise due to recent global warming (IPCC AR, 2014). The glacier are mostly formed in the conditions with high snowfall in winter and cool temperature is summer which is highly favorable in polar and high alpine regions. The continental glaciers maintain the earth temperature by absorbing impending solar radiation whereas mountain (alpine) glaciers contributes to river flow thus maintaining livelihoods in riparian area during dry season. Both the glaciers behave differently to deal with other climatic parameters to maintain hydrological cycle in atmosphere (WWF, 2005).

The fluctuation in glaciers provides clear evidence of climate change in regional and global scale which is a natural phenomenon that has been occurring in the Earth's long history (Zemp and others, 2016). These melting glacier have direct impacts on available water resources, impending natural hazards, sea level rise and other socio-economic consequences. The precipitation and temperature pattern greatly influences the behavior of glaciers which nourishes the rivers downstream. In the past few decades, global climate change has had a significant impact on the high mountain environment: snow, glaciers and permafrost are especially sensitive to changes in atmospheric conditions because of their proximity to melting conditions (UNEP, 2010). In fact, changes in ice occurrences and corresponding impacts on physical high-mountain systems could be among the most directly visible signals of global warming. This is also one of the primary reasons why glacier observations have been used for climate system monitoring for many years.

1.2 Himalayan glaciers and regional shrinkage

Climate change and its impact on variation of Himalayan glaciers is a natural phenomenon that has been occurring since many years in Himalaya. Glaciers in those region, are one of the

major source of water and mostly neglected by scientific community, feed 1.4 billion of population in its vicinity area (Bajracharya, 2014a). After publication of IPCC AR5 report, nevertheless, it has gained tremendous attention to national governments, scientific community and other concerned stakeholders.

Himalayan glaciers play eminent role in maintaining regional water resources and regarded as a most visible indicators of climate change in South Asian region (Immerzeel, 2010, Kaser, 2010, Bolch, 2012). Continuous shrinkages of those ice mass during the last couple of decades drew serious attention to scientific community, local authority and other concerned stakeholders. Mid-eastern Nepal Himalaya, mostly covered with high altitude glaciers has high behavioral uncertainties owing to lack of proper in-situ monitoring, inaccessible terrain and poor economic region (Cogley, 2010, Bagla, 2009). Thus, more scientific investigations are urgently realized in those unexplored water towers to ascertain potential changes in glaciers mass and its future behavior.

In Himalayan region, previous studies on glacier shrinkage are scarcely available and most of them are confined either in Everest region or in low altitude area which totally does not reflect the real ground conditions. For example, Shangguan, 2014 reported high glaciers shrinkage (19 ± 5.6%) in Koshi basin and losses are more pronounced in Southern flank as compared to Northern flank of Mount Everest region. Similar study conducted by Thakuri, 2014 investigated 400 km^2 of glacier in Everest region over the last five decades (1960 – 2011) and showed overall surface area loss of 13.0 ± 3.1%. In the broader scale study by Bajracharya, 2014a found 24% glaciers area loss over the last three decades (1980 – 2010). On the other hand, apparent mass changes of -0.32 ± 0.08, -0.40 ± 0.25 and -0.16 ± 0.16 m w.e. a^{-1} were reported in the Khumbu region by Bolch and other, 2011, Nuimura and others, 2012 and Gardelle and others, 2013, respectively. All of the research mentioned above are confined to small geographical extent and mostly used with coarse resolution Landsat images which demands the regional scale study by using fine resolution satellite images.

On the other hand, debris covered glacier has suspicious behavior to climate (Scherler and others 2011a, Fujita and Sakai, 2014), which gives ample opportunities to work further in this part of the world. Most of the glaciers in this area are covered with supraglacial debris which

tend to melt at slower rate than that of debris free ice owing to its insulating properties (Hambrey, 2008).

But all of the studies mentioned above was mostly confined to small region and used coarse resolution remote sensing images which demands regional scale monitoring using high resolution data.

1.3 Aim of this study

As we noticed, most of the previous researches were focused on Everest region; the main purpose of this study to investigate glaciers in regional scale. This study covers from Bhutan in the east to the Langtang in the west considering the national territory of Bhutan, India, China and Nepal and on both sides of Himalayan barrier. The main aim of this study is to investigate regional glaciers with high resolution satellite observations. To accomplish the main goal, we set following objectives in three folds:

(a) To create novel glacier inventory with high resolution ALOS images in regional scale

(b) To assess decadal glacier shrinkage and compare with other studies in broader scale

(c) To quantify debris part of the glacier and investigate the reason behind its formation.

This thesis consist of four chapters: Chapter 2 deals with study area and the climate trends in Himalaya. The methodology used during this study has been elaborated in Chapter 3 where we present about data acquisition, processing, delineation and accuracy. The results and discussions section in Chapter 4 quantifies number and area of glaciers and its regional shrinkage. And in Chapter 5, we conclude our study and present some recommendations for upcoming research.

2. GEOGRAPHICAL EXTENT AND CLIMATE SETTINGS

2.1 Study area

Nepal, located in the central domain of Himalaya, has 3,808 glaciers covering nearly 3,902 km2 (Bajracharya et al., 2014a). Our study area, located in mid–eastern part of Nepal Himalaya, extends from Bhutan in the east to Ganesh Himal in the west (88º10″ E, 28º30″ N) (Fig. 1a). In this study, entire area is further divided into four massifs; namely Langtang (LT), Khumbu (KB), Kanchenjunga-Sikkim (KS) and Bhutan (BT) covering geographical territory of Nepal, Bhutan, India and China in both sides of Himalayan barrier. Most of our research is carried out in wider

region from LT in the west to BT in the east expect decadal shrinkage analysis which is confined to Nepal territory because of available data restrictions.

In the first part of this study, we delineated glacier inventory for both debris-free (C-glacier hereafter) and debris-covered (D-glacier hereafter) glaciers and their spatial distribution from LT in the west to BT in the east. Secondly, we check the relation between debris cover extension and their corresponding potential debris supply (PDS) across the whole region. And lastly, our decadal shrinkage analysis is limited to Nepal territory due to data restrictions. To understand the role of mountain peaks over the formation of debris cover extent, we again separate glaciers into the southern-side (S-glaciers hereafter) and northern-side (N-glaciers hereafter) considering mountain as a climatic barriers. This geographical separation almost follows political boundary of neighboring nations expect few areas in western massifs (Fig. 1b).

2.2 Climate in Himalaya

Climate settings in eastern Himalayas is mainly governed by the fluctuation of precipitation and temperature. Eastern Nepal is mainly dominated with onset of Indian monsoon from Bay of Bangal and is regarded as main source of glacier accumulation (Fujita and Ageta, 2000). The majority of annual rainfall, approximately 77 % (Wagnon and others, 2013), occurs between June and October, with decrease from east to west and south to northwest (Bookhagen and Burbank, 2010, Shrestha and others, 2000). Recent study by Sakai and others (2015) showed high contribution of precipitation to glaciers mass accumulation in Hindu Kush, the Himalayas and the Hengduan Shan as compared to western arid mountains. The daily mean temperature at 5000 m elevation, where most of the glaciers are located, ranges between −7 to +10 °C, with minimum and maximum daily temperatures ranging between −25 and +10 °C whereas during monsoon period between June to September, temperature are generally above 0 °C with low variability (Shea and others, 2015). Salerno et al., 2014 recently examined seven weather stations located between 2660 and 5600 m a.s.l over last two decades (1994−2013) in southern slope of Mr. Everest region and concluded that weak precipitation and warm winters are the major source of glacier melting.

The Southern face of eastern Nepal Himalaya mostly dominated with debris mental (Scherler and others, 2011b), receive summer precipitation from South Asian monsoon whereas winter

precipitation from westerly wind mainly dominates western Himalayas (Ageta and Higuchi, 1984).

3. METHODOLOGY

3.1 Glacier inventories

3.1.1 ALOS glacier inventory

New glaciers outlines were delineated with the help of 2.5 m Panchromatic Remote-sensing Instrument for Stereo Mapping (PRISM) and Advanced Visible and Near Infrared Radiometer type 2 (AVNIR-2) onboard Advanced Land Observing Satellite "DAICHI" (ALOS) which was launched on January 24, 2006. Out of 1536 available images for this study area, 104 images (Table: 1 and Fig: 1b) were carefully selected to avoid high cloud cover and heavy snow cover and mostly taken from post monsoon period of that particular year. Most of those images were ortho-rectified with a PRISM-derived digital surface model using "DSM and Ortho-image Generation Software for ALOS PRISM (DOGS-AP)" (Tadono and others, 2012). Some of the ALOS PRISM images ("*" in Table: 1) were orthorectified by using Leica Photogrammetric Suite (LPS – 2011) with the aid of Rational Polynomial Coefficient (RPC) as orientation parameters (interior and exterior information) and ASTER GDEM 2 as elevation data source. All together 5301 glaciers including D-glaciers and C-glaciers were delineated by using ALOS images between 2006 – 2011 and among them majority of glaciers were delineated with high resolution 2.5 m ALOS PRISM whereas only few were delineated based on 10 m AVNIR-2 images. We assure that this as a first inventory prepared with such a high resolution satellite images covering whole mid-eastern Nepal Himalaya.

Various topographical parameters such as glacier area, contour lines, slope and aspect were derived with the help of widely used global elevation model generated from the Advanced Spaceborne Thermal Emission and Reflection Radiometer, version 2 (ASTER GDEM-2). The slope map and contour map produced with ASTER GDEM-2 were also used during glacier delineation when shadow zone was encountered. The main reasons behind using ASTER GDEM-2 over Shuttle Radar Topography Mission (SRTM) DEM are because of its high spatial resolution of 30 m and higher accuracy in high mountain region (Tachikawa and others, 2011, Bolch and others, 2011). ASTER GDEM-2 has an upper hand over SRTM in terms of accuracy

in high and steep mountains (Luedeling and others, 2007, Reuter and others, 2006) and has lower bias of +40 m (Nuimura and others, 2015). This product is already applied successfully by Sakai and others, 2015 and Nuimura and others, 2015 for glacier investigation in high mountain Asia.

3.1.2 1992 glacier inventory

Supraglacial debris in ablation areas, orographic steepness surrounding the glaciers and snow cover are the major factors that hinder glacier mapping using satellite imageries in the Himalayas. Compared to automatic mapping or tracing over topographical maps, manual delineation from aerial photograph interpretation is a more reliable method of producing complete and accurate glaciers inventory (Asahi K, 1999).

In this study, glaciers were identified by the visual interpretation of 406 vertical aerial photographs taken in 1992 by Survey Department of Nepal. Glaciers delineation from aerial photographs were carried out with the aid of stereoscope at Department of Hydrology and Meteorology (DHM), Nepal from June 1996 until May 1997 by the group led by Dr. Katsuhiko Asahi. Topographical sheets of scale 1:50,000 were used as base map which were produced with the same aerial photographs. Main advantage of using stereoscope in mapping glaciers with aerial photographs are, firstly glaciers can be recognized as a three-dimensional cubic volume, making it possible to separate glacier ice from snow, and secondly, debris part can also be seen clearly in glacier's terminus. The details of aerial photographs used in this study are described in Table 2.

The Landsat 5 Thematic Mapper (TM) images, freely downloaded from http://landsat.usgs.gov/, were used to cross-examine and validate 1992 inventory derived with aerial photographs and also to confirm number of vanished glaciers during the study period. Those images were also taken during post-monsoon time (end of the ablation period) to reduce uncertainties related to seasonal snow cover (Table: 1).

3.1.3 Other glacier inventories

Comparison of ALOS inventory, in terms of number and area, to other inventories is one of the secondary objective of this study, as we suppose large number of small glaciers were not enumerated in other inventories due to the limitation of coursed-resolution data set used. In our study we compared ALOS inventory with both GAMDAM inventory (GGI, Nuimura and others,

2015) and ICIMOD inventory (Bajracharya and others, 2014a) as both of these inventories largely cover our study region. We also incorporated ALOS-based Bhutan inventory (Nagai and others, 2016) to understand longitudinal behavior of glacier formation. Other inventories with some limitations are also available in this region; namely Chinese glacier inventory (CGI, Guo and others, 2015) and Randolph glacier inventory (RGI, Pfeffer and others, 2014). The main drawback of CGI is its aerial coverage which is only confined to China political territory and offers less coverage to our overall study area. On the other hand, the reason behind not using RGI version 5.0 (released on 20th July, 2015) is due to its combination of CGI (in Chinese territory) and GGI (in Nepal, Bhutan and India territory) of mid-eastern Himalaya as both CGI and GGI differ in the way of delineation particularly in upper boundary case.

GAMDAM inventory was generated based on 356 Landsat ETM+ scenes taken during 1999-2003 and with the aid of digital elevation model (DEM) and high resolution Google Earth^{TM} (Nuimura and others, 2015). It revealed 87,084 glaciers covering a total area of 91,263 ± 13,689 km^2 over high mountain Asia which is slightly lesser than ICIMOD inventory in terms of area of the same region. On the other hand, latest ICIMOD inventory published in 2014 were based on semi-automatic delineation and used Landsat-5/-7 from the period of 1977-1978, 1990, 2000 and 2010 (Bajracharya and others, 2014a). In our study, we used ICIMOD inventory from 2010 in which glacier ice was identified based on threshold of normalised difference snow index (NDSI).

3.2 Manual delineation

Despite semi-automatic glacier mapping being moderately accurate for clean ice, it needs significant manual correction mostly in large part of debris cover and shadow zone (Paul and others, 2013). In our study sites, glaciers are largely dominated by debris-covered type and high shadow zone owing to high relief, we preferred to opt manual delineation method instead of semi-automatic. To ensure accurate glacier delineation, not only the same source of images with high spatial resolution were utilized, but also a single operator was engaged in glacier mapping (for a six month) to minimize personal differences among users as recommended by Global Land Ice Measurements from Space (GLIMS) workshop held in June, 2008 (Racoviteanu and others, 2009). Glacier polygons were carefully delineated as per guidelines provided by GLIMS (Raup and others, 2010, Rastner and others, 2012, Nagai and others, 2013). Glaciers divides were identified with the help of 20 m contour map generated with ASTER GDEM 2. The delineated

glacier polygons were overlaid on Google Earth™ to check its accuracy for further improvement and corrections were also made after consultation with experienced lab members especially in difficult areas (shadow zones, glacier divides and debris part).

To understand the climatic behavior on different types of glaciers, we discriminated the glaciers as C-type and D-type glaciers. On top of that, we again separated debris-free part (hereafter "C-part) and debris-covered part (hereafter "D-part") to understand influence of PDS on debris cover extension (Fig. 2). We assure no previous studies ever documented the extent of C-part and D-part of glaciers over regional scale in this part of Himalaya.

3.3 Delineation error

Many technical factors such as resolution of data, use of different sensors and image processing techniques affect the proper delineation of glaciers. At the same time other non-technical errors, for example, human error during delineation, different perceptions on glacier boundary (definition error) especially towards glacier head on steep mountains may add significant error in glaciers mapping. Even though the images used in this study have very high resolution and those data were carefully selected to avoid seasonal snow and cloud cover, some of the systematic and non-systematic errors mentioned earlier may still contain in the glacier inventories that need to be estimated for assessing accuracy of the produced maps. While various methodologies are available for error estimations, the uncertainties of glacier delineation were calculated following the methodology proposed by Nagai and others (2016) in the Bhutan Himalaya because our study has similar topography, the same climate, and the same data quality. In Nagai and others (2016), two different empirical equations for C-type glaciers ($y = 30.5\ x^{-0.19}$) and for D-type glaciers ($y = 7.54\ x^{-0.12}$) were generated based on multiple digitization of variously sized glaciers by four operators; where x denotes the size of glaciers and y denotes the uncertainty associated with it.

3.4 Georefrencing of ALOS and 1992 inventory

To ascertain actual glacier shrinkage, we need to overlap ALOS inventory on top of 1992 inventory to match both the inventories. As mentioned earlier, 1992 inventory was prepared with the help of vertical aerial photographs of 1:50,000 scale and later stereoscopically corrected to decide three-dimensional exact position. Topography map with 1:50,000 scale were used as a

base map. Altogether 102 ground control points (GCPs) including mountain peaks and river crossings were identified and embedded along with 1992 glaciers inventory. To use 1992 inventory in conjunction with newly build ALOS inventory, we need to align or georeference 1992 inventory with ALOS images having known coordinate system. The georefrencing process involves identifying a series of ground control points (i.e. known x, y coordinates) in ALOS images which can be linked with GCPs embedded in 1992 inventory. All together 73 clear and distinct GCPs were identified in ALOS images and linked to corresponding GCPs in 1992 inventory in ArcGIS 10.2 with georefrencing tools. Total root mean square Error (RMSE) during registration was obtained as minimal as possible by considering more number of GCPs.

3.5 Tropical Rainfall Measurement Mission (TRMM)

To understand the relationship between the glacier distribution and the climatic parameter, we used Tropical Rainfall Measurement Mission (TRMM) Multi-satellite Precipitation Analysis (TMPA) for precipitation data over the Himalayas. The TRMM-derived precipitation data has already employed in many parts of Himalaya and found useful in understanding climate dynamics (Houze and others, 2007, Shrestha and others, 2012). In particularly, Bookhagen and others, 2006 confirmed two distinct rainfall maxima along strike in the Himalaya by using both passive microwave radiometer (TMI) and active precipitation radar (PR). Other comparative study carried out by Yamamoto et al., 2011 in Khumbu region reported high consistencies of TRMM products to in situ measurements as compared with other products. Nagai et al., 2016 also tested TMPA data over Bhutan Himalaya and found slight relationship between debris cover extent and TRMM-derived precipitation. To analyse in broader scale, in our study, we processed monthly product (TRMM 3B43) and averaged for the period 1998–2012 to obtain mean annual precipitation data.

3.6 Potential debris supply (PDS)

The concept of potential debris supply (PDS) slopes was proposed by Nagai et al, 2013 for Bhutan Himalaya which is followed here to understand regional influence of local topography to D-part formation. The PDS is the slope that could supply the debris mantle into the glaciers as a rock fall or as an avalanches, which has been digitized manually as the continuous slope between glacier boundary and mountain crest. The mountain ridge was confirmed by using 20 m contour map and slope map generated from ASTER GDEM2 (Fig. 2). The slopes interrupted by hills or

lateral moraines are excluded from PDS slopes as debris in prevented by depression to reach into the glaciers whereas slopes of lateral moraines were included if they are inclined towards glacier surface. Furthermore, those polygons were checked against Google Earth™ for quality improvement.

4. RESULTS AND DISCUSSIONS

4.1 ALOS derived glacier inventory

4.1.1 Area, number and other attributes

The study area surrounds 5301 glaciers with a total area of 5691±893 km^2, where 4459 C-glacier covering the area of 1852±140 km^2 (0.42 km^2 per glacier) and 842 D-glacier covering the area of 3838±752 km^2 (4.6 km^2 per glacier) are identified (Table 3, Fig. 1a). This ALOS inventory covers 6 %, both in terms of number and area, of the glaciers that contained in whole high mountain Asia previously estimated by Nuimura et al., 2015. The C-glaciers in this region are strongly right-skewed confirming large domination of small size C-glaciers whereas D-glaciers are symmetrically distributed over different glacier sizes (Fig. 3). The cumulative area for D-glacier is almost double than that of C-glaciers. The median area of glaciers (0.1 km^2 for C-glacier and 1.5 km^2 for D-glacier) are much lower than their respective mean area (0.4 km^2 for C-glacier and 4.5 km^2 for D-glacier) confirming large number of glaciers belonging to smaller size.

To understand the dynamics of D-part extension across the Himalayan, we divide our study area into two separate zones considering mountain peaks as a climatic barrier. We find 2220 glaciers covering the area of 2636 ± 397 km^2 are situated in northern side (hereafter "N-glaciers") and 3081 glaciers covering the area of 3054±495 km^2 are situated in southern side (hereafter "S-glaciers") of the mountain barrier. Although the glaciers across mountain barrier has similar slope feature, the glaciers situated in southern side has maximum coverage at lower elevation zones than that of northern side giving median elevation of 5464.9±340.5 m and 5801.8±399.4 m a.s.l., respectively.

Although the hypsometry of D-glaciers has wider distribution over C-glaciers, both glaciers has their maximum area in similar elevation band. The median elevation of glaciers in

this region is found to be 5605.2±402.3 m a.s.l where D-glaciers (5484.3±369.2 m a.s.l.) are clearly situated in lower elevation than C-glaciers (5627.9±404.5 m a.s.l.). The mean slope of these glaciers is 30.1±8.6°, where D-glaciers (26.8±6.9°) are distinctly flatter than C-glaciers (30.7±8.8°) due to its high tendency to spread over large elevation range (Table 3).

4.1.2 D-part extension over the region

The scientific understanding of debris covered glaciers in this part of Himalaya is largely scarce, which motivates us to quantify D-part and analyse its regional existence. The 842 D-glaciers are further separated as C-part and D-part by inspecting multiple images of similar time period. The C-part area ranges from 0.01 to 80.9 km^2 (mean area of 3.4 km^2) whereas D-part area ranges from 0.01 to 27.2 km^2 (mean area 1.2 km^2) totalling the area of 2867±167 km^2 and 971±236 km^2, respectively.

The C-part and D-part of debris covered glaciers show distinct separation of their maximum area in upper and lower elevation modes, giving median elevation of 5608±335.6 m and 5197.6±358.2 m a.s.l. (Table 3), respectively. Interestingly, we find that the C-part of debris glacier is hypsometrically identical to C-type glaciers below 5400 m elevation. The average slope of D-part (22.0±8.6°) is much lower than its corresponding C-part (30.2±8.0°).

4.2 Intra-regional statistics of glaciers

4.2.1 C- and D-glaciers

The far-western LT massif has lower cluster of glaciers, both in terms of area and number, as compared to other three eastern massifs (Fig. 1a, Table 3). Overall, the massifs are largely dominated by D-glacier (67 % in total) with largest coverage in KB region (73%) and found to be declining towards eastern massifs for instance in KS (65%) and BT (61%) resulting increment in C-glaciers coverage towards east. Consequently, the D-part coverage (%) is also found to be declining from west to east for instance: LT (29%), KB (27%), KS (23%) and BT (23%) resulting increment of C-part coverage towards east.

4.2.2 Area-elevation distribution

The most of the glaciers in the study area are situated between 5000 to 6500 m a.s.l. The maximum coverage of BT and LT massif are situated distinctly at lower elevation zone (5400–5500 m a.s.l.) whereas KB and KS massifs shows its maximum coverage at slightly higher elevation zones (5700–5800 m a.s.l.). The hypsometry of C-glaciers clearly shows larger coverage in BT massif in lower elevation zone (5400–5500 m a.s.l.), whereas symmetrical distribution of glaciers is found in case of D-glaciers. Although similar altitudinal profile is found in lower elevation zone (below 5000 m a.s.l.), widely varied distribution of glaciers is noticed in upper elevation zone (above 5000 m a.s.l.) for both C- and D-glaciers. The hypsometry of D-part coverage is distinctly situated in lower elevation mode. Although both C-part and D-part shows similar altitudinal profile below 5400 m a.s.l. and 5000 m a.s.l. elevation, respectively, the glacier distribution in upper elevation is widely varied for both and noticeably higher in KB massif.

4.2.3 Regional elevations and slopes

Since all the massifs show identical elevation range from west to east, we further carried out statistical analysis (student t-test) between different elevations and longitude (based in area weighed at 0.25˚grid) to investigate regional differences among the massifs. We find that the maximum elevation of the glaciers decreases ($r=-0.40$, $p=0.03$) from west to east on contrary to its median ($r=0.29$, $p=0.1$) and minimum ($r=0.31$, $p=0.09$) elevation which increases from west to east making elevation range slightly narrower towards west. The median elevation of D-glaciers are clearly situated in lower elevation than that of C-glaciers especially in western massifs (LT and KB), whereas eastern massifs (KS and BT) depict similar median elevation for both types of glaciers. The statistical analysis shows that the median elevation of C-glaciers has decreasing trend ($r=-0.25$, $p=0.1$) towards east, whereas no significant trend is found for D-glaciers implying median elevation for D-glaciers is stable throughout the study area. On the other hand, the median elevation of S-glaciers are distinctly in lower elevation zone than that of N-glaciers across the Himalayan barrier. On regional scale, we find significant decreasing trend ($r=-0.48$, $p=0.01$) of median elevation from west to east in southern-side of the mountain barrier whereas no trend is found in northern-side concluding stable nature of glaciers across the mountain.

Over the region, the glaciers slope is found to be significantly decreasing (r=–0.45, p=0.01) from west to east. Although D-glaciers are comparatively flatter than C-glaciers because of its larger size and tendency to spread over wider elevation range, both glacier has a decreasing slope towards east i.e. r=–0.47 (p=0.01) for D-glacier and r=–0.47 (p=0.009) for C-glacier.

4.3 Comparison between the multiple glaciers inventory

Although AGI shows more number of glaciers (5301) as compared to GGI (4526) and IGI (4690) due to fine resolution (2.5 m) images used during delineation, the total areal coverage (5691±893 km^2) is found to be smaller than IGI (6211 km^2) but larger than GGI (5422 km^2). These three inventories show similar altitudinal distribution, the main discrepancy between AGI and GGI is found to be in higher elevation zone, where GGI is underestimated due to its slope limitation in upper glacier boundary during delineation. IGI inventory overestimates in all elevation zones than other two inventories.

4.4 Decadal glacier shrinkage

4.4.1 Glacier shrinkage in mid-eastern Nepal Himalaya

Among glaciers, which are exactly matched in the ALOS and 1992 inventories, the total area of glaciers decreased from 1616 ± 247 km^2 in the 1992 inventory to 1477 ± 232 km^2 in the ALOS inventory, giving –8.5% area change (–0.5±0.1 % a^{-1}) during the study period. Slight increment in number of glaciers from 1066 to 1142 (7%) was resulted from disintegration of glacier, which has also been reported previously in the Nepal and Bhutan Himalayas by Bajracharya and others (2014a, b).

The hypsometry diagram shows that both types of glaciers have shrank noticeably in the lower elevation below 5750 and 5950 m a.s.l. for C-type and D-type glaciers, respectively based on third quartiles of area change. Shrinking patterns are similar in both types of glaciers; the maximum area of shrinkage is found at the almost same elevation, i.e. 6.5 km^2 at 5400-5500 m a.s.l. for the C-type glaciers and 7.9 km^2 at 5200-5300 m a.s.l. for the D-type glaciers. We clearly notice elevation range corresponding to maximum area for glacier change are slightly lower than the existing glaciers for both C-type and D-type glaciers.

Small C-type glaciers (< 1 km^2), which are predominantly large in number, have lost larger portion of their area; i.e. more than 40% in many cases whereas medium and large C-type glaciers (> 1 km^2) have lost less portion (~20%) of its area. Likewise, small D-type glaciers (<10 km^2) have lost larger portion of its area as compared to large D-type glaciers (>10 km^2) which are confined to less than 20%. In terms of absolute area, small-sized glaciers (< 1 km^2) have changed less average absolute area (0.05 ± 0.05 km^2) as compared to large and medium sized glaciers (> 1 km^2), which have lost average absolute area of 0.17 ± 0.13 km^2 for the C-type glaciers. The average absolute area changed for the D-type small-sized glaciers (<10 km^2) is 0.20 ± 0.31 km^2 and for medium and large size glaciers (>10 km^2) is 1.81 ± 1.75 km^2.

4.4.2 Completely disappeared glaciers

No previous study has reported about complete disappearance of glaciers in the eastern Nepal Himalaya so far. To cross-examine existence of glaciers and their topographical orientation, we utilize four Landsat TM images taken during the post monsoon season of 1992 (Table 1) and overlaid with the 1992 glacier inventory. In total, 61 (5% of total number) C-type small-sized glaciers covering the total area of 2.4 ± 0.3 km^2 (0.1 % of the total area), which ranged from 0.01 to 0.20 km^2 (average size of 0.04 km^2), have completely disappeared during the study period. This value is comparatively lesser than the Northern Patagonia, where 374 small-sized glaciers (< 0.50 km^2) out of 1664 have been found completely disappeared (22% of total number) between 1985 and 2011 (Paul and Mölg, 2014). Within the study region, Ganesh (14) and Khumbu (34) are the massifs in which relatively large number of glaciers have disappeared since 1992; covering area of -0.7 ± 0.1 km^2 and -1.2 ± 0.1 km^2, respectively.

4.4.3 Comparative study of glacier shrinkage

Previous studies have reported widely ranging rates of area change in glaciers along the Himalayas and neighbouring regions over a couple of decades (Fig. 4). For instance, Ye and others (2006) and Yao and others (2012) showed relatively less rates of area change in glaciers on the Tibetan Plateau (TP) ccompared with those in the Nepal (NH) and Bhutan (BH) Himalayas, where most of glaciers were facing southward (Bajracharya and others, 2014a). Kulkarni and others (2007, 2011) found that glaciers in the western Indian Himalaya (IH) have changed with rates of –0.54 and –0.41% a^{-1}, which were significantly more negative than that in

the eastern Sikkim Himalaya (SK-IH, –0.16% a^{-1}, Basnett and others, 2013) and in Kanchenjunga-Sikkim area (KJ-NH, –0.23% a^{-1}, Racoviteanu and others, 2015). On the other hand, significant discrepancy was found in the Bhutan Himalaya (BH), in which Karma and others (2003) reported less negative rate of area change (–0.27% a^{-1}) than that (–0.78% a^{-1}) reported recently by Bajracharya and others (2014b). Such a significant discrepancy may be due to difference in data quality used and study period. As toposheets (1:50,000) produced in the 1960s and SPOT images (20 m resolution) taken in December 1993 were used in the study by Karma and others (2003) whereas only Landsat images (1980-2010) were used in the study by Bajracharya and others (2014b). Large uncertainty in the 1960s toposheets may be the main source of the significant discrepancy though the recent acceleration of glacier shrinkage may be also contained in the difference. Nie and others (2010) investigated both southern (ES-NH) and northern (EN-NH) slopes of the Everest region by producing glacier extent based on Normalized Difference Snow/Ice Index (NDSII), and found slightly more rapid shrinking in the southern flank (–0.56% a^{-1}) than in the northern flank (–0.48% a^{-1}). Bolch and others (2008) investigated glaciers in the Khumbu region based on multitemporal imageries taken in 1962 (Corona KH-4), 1992 (Landsat TM) and 2005 (Terra ASTER), and reported much less negative area change (–0.12% a^{-1}) among those compared above. Recent studies carried out in the Khumbu region reported contradictory rates of area change such as –0.27% a^{-1} (1962-2011, Thakuri and others, 2014) and –0.58% a^{-1} (1976-2009, Shangguan and others, 2014) though the analyzed periods are similar. Even though both the glacier outlines were manually digitized, one of the reason behind double rate of shrinking reported by Shangguan and others (2014) may be due to data quality, as toposheets (1:50,000 and 1:100,000) were used for the glacier outlines in 1971-1980. Unlike the other studies, which enumerated overall glaciers, the present our study reports categorical shrinking rates of –0.50% a^{-1}, –0.47% a^{-1} and –0.70% a^{-1} for overall, D-type and C-type glaciers, respectively. Comparing with the other studies, this study yields similar rate of area change (–0.50% a^{-1}) as compared to –0.56% a^{-1} reported by Nie and others (2010) for the overall glaciers while considerably greater area loss (–0.70% a^{-1}) is reported for the C-type glaciers (as compared to –0.24% a^{-1} by Bolch and others, 2008) because the C-type glaciers are expected to have exhibited higher area loss than the D-type glaciers (Scherler and others, 2011). Another reason may be our investigation period, which is shorter and in more recent decades, during

which glacier shrinkage was accelerated in many part of High Mountain Asia except for the Karakorum (Gardelle and others, 2013).

4.4.4 Spatial distribution of glacier shrinkage

The spatial distribution of area change for the C-type glaciers in the east Nepal Himalaya ranges from –0.01 to –0.80 km^2 (average of –0.06 km^2) and totalling 54.3 km^2 at the rate of –0.7% a^{-1} during the studied period. The entire domain is largely dominated by small area change with some exceptions of larger change. We also analyse intra-regional pattern of the area change in the four massifs (Fig. 5). The glaciers in the Ganesh massif shows noticeably more negative (greater loss) area change (median value of –0.08 km^2) than Langtang (median value of –0.04 km^2), Khumbu (median value of –0.04 km^2) and Kanchenjunga (median value of –0.03 km^2) massifs. Although number of glaciers is less (44) in the Ganesh massif, difference of the area change is statistically significant ($p < 0.0001$ by t-test). The reason behind glaciers in the Ganesh massif are so vulnerable may be due to its location; glaciers in the Ganesh massif are located at relatively lower elevation as compared to the other Langtang, Kangchenjunga and Khumbu massifs where relatively higher temperature is expected during summer melting season. Another plausible reason is its slope; as glaciers in Ganesh massif stay steeper than the other massifs. Similar results, in which steeper glaciers lost larger area, were reported in the Kanchenjunga-Sikkim region ($r=0.47$, $p = 0.01$, Racoviteanu and others, 2015) and in the Khumbu region ($r2=0.21$, $p <0.01$, Salerno and others, 2008).

4.4.5 Area loss and topographical settings

The area change of glaciers in the studied domain is examined with topographical variables such as elevations and slope in terms of Pearson's correlation coefficient. Aspect is not examined because the study domain is limited within the Nepal territory and thus biased toward south. Moderate but significant correlation is found between the area change and the minimum elevation ($r = 0.30$, $p < 0.0001$), indicating that glaciers situated at lower elevation have lost more area. The most significant negative correlations of the area change are found with elevation range ($r = –0.50$, $p<0.0001$) and glaciers size ($r = –0.62$, $p < 0.001$), suggesting that larger glacier lost larger area. A week but significant correlation of area change is also found with mean slope ($r = 0.16$, $p < 0.0001$), which might be resulted from larger glacier tending to have gentler slope which are mostly covered with supraglacial debris resulting weak correlation.

4.5 Potential debris supply controls debris extension in Himalayas

4.5.1 Relation between D-part and PDS slopes

The significant positive correlation is found between debris part of the glaciers and its corresponding PDS area implying larger PDS area tends to supply larger debris mantle into the glaciers (Fig. 6). The relation is strong in all massifs for example in LT ($r=0.94$, $p<0.0001$), KB ($r=0.88$, $p<0.0001$), KS ($r=0.94$, $p<0.0001$) and BT ($r=0.80$, $p<0.0001$). Stronger correlation in western massifs is owing to larger PDS area and steeper PDS slope in western massif which tend to yield sufficient supraglacial debris mantle into the glaciers.

We further analyse glaciers from two separate groups across the mountain barrier; namely N- and S-glaciers and establish the relation of D-part area against their corresponding PDS area. The S-glaciers clearly shows high correlation value than that of northern-side glaciers except LT massif. Both sides of glaciers show strong positive correlation between their D-part and corresponding PDS slope, resulting that N-glaciers have smaller D-part area than S-glaciers for their corresponding PDS area, except in KB massif. Therefore, we further analyse south-facing PDS slopes (90°–270°, clockwise) and correlate D-part area with its corresponding PDS area. The correlation between south-facing PDS slope and D-part area is improved (0.86, $p<0.0001$) than that for the total PDS area ($r=0.80$, $p < 0.0001$) in far-eastern BT massif and improvement is weakening toward west. In far-western LT massif, the correlation coefficient demote for both south-facing PDS slope ($r=0.88$, $p<0.0001$) and north-facing PDS slope ($r=0.89$, $p<0.0001$) than that of total PDS area ($r=0.94$, $p<0.0001$).

4.5.2 Effect of PDS aspect and PDS gradient to debris-part formation

In order to understand the effect of PDS orientation and gradient to D-part formation, we further established correlation coefficient between D-part area and its corresponding PDS aspect and PDS gradient for glaciers situated in both southern and northern-side of Himalayan barrier.

Figures 6a and 6b show the correlation coefficients between the PDS slope area and corresponding D-part area for S-glaciers and N-glaciers, in different aspects. Higher correlation was found in southern-side than that of northern-side glaciers. Although high correlation values was found for different aspect in different massif (for example in southern-side: W for Langtang, SW for Khumbu, SE for Kan-Sikkim and SW for Bhutan), the correlation are associated with its

corresponding PDS area coverage (%). That means larger PDS coverage (%) from SE to W tends to supply larger debris mantle into the glaciers. Similarly, good association (decreasing trend from N to NW clockwise) between correlation coefficient and corresponding PDS coverage was found in northern-side glaciers as well.

In terms of PDS gradient, the PDS area having slope less than 70° are highly responsible for D-part formation and more pronounced in southern-side (Fig. 6c and 6d). The correlation coefficient is found to be decreasing after 70° which corresponds to decreasing PDS area coverage (%). The lower correlation value in northern-side of Himalayan barrier is due to presence of larger snow coverage in its accumulation zone; as flatter slope is expected with larger snow coverage and tend to produce lesser debris mantle. On contrary, high rocky mountain with less snow coverage and steep slope in southern-side tend to produce high frequency of rock falls and avalanches. Although 25% of PDS area lies in 50°-60° in southern-side and 40°-60° in northern-side, no evident correlation was found in that particular slope range.

5. CONCLUSIONS AND RECOMMENDATIONS

We manually digitized 5301 glaciers (5691 ± 893 km^2) on both sides of mountain barrier in Mid-eastern Himalaya range covering the political territory of Bhutan, India, China and Nepal using 104 high resolution (2.5 m) ALOS-PRISM images. Among those glaciers, 4459 C and 842 D-type glaciers covering the area of 1852 ± 140 km^2 and 3838 ± 752 km^2, respectively, were found to be spread over the four massifs. Over the region, 971 ± 236 km^2 of glacier is completely covered with debris mantle which was not previously documented. The regional elevation profile shows that the glaciers situated in southern slope of mountain barrier are relatively in lower elevation zone than that situated in northern slope. The statistical analysis carried out in four massifs depicted lowering of median elevation from west to east making elevation range narrower towards east.

Among 5301 glaciers delineated for this study, 1290 glaciers which are situated in Nepal political territory is compared with another set of glacier polygons created with aerial photographs taken in 1992. As previous studies were limited within the Everest region, this study expanded the coverage investigated from Ganesh in the west to Kanchenjunga in the east, and analyzed both C-type and D-type glaciers. The entire domain showed large rate of glacier

shrinkage; –0.5 % a^{-1} for the whole glaciers, –0.47 % a^{-1} for the D-type glaciers and –0.7 % a^{-1} for the C-type glaciers, respectively, since 1992. Our study showed comparatively larger rate of shrinking over east Nepal Himalaya as compared to its vicinity areas. Smaller glaciers, especially C-type, are losing its large portion of area as compared to the larger glaciers. Intra-regional analysis showed statistically significant high rate of shrinking in the Ganesh massif located in the west than the other eastern massifs, which is one of the interesting findings of this study. Significant number of small-sized glaciers (covering area of 2.4 km^2) were found to have been completely disappeared since 1992, which were not reported so far in the Nepal Himalaya. Though climate interpretation was not the scope of this study, recent alternation in temperature and precipitation could be the plausible explanation behind the glacier shrinkage, which needs further investigations as more and more ground observations are available.

On the other hand, the D-type glaciers from entire domain were further divided into D-part and C-part to examine the regional dynamics of debris-covered glacier formation. The concept proposed by Nagai et al., 2013, to understand the plausible cause of D-part formation with relation to its PDS source, was adopted and extended in larger spatial domain. We found significant positive correlation between PDS and D-part area implying that larger PDS area tend to produce larger debris mantle onto the glaciers. The relation is slightly strong in western massif than that of eastern one, which could be owing to its larger PDS area and steeper slope. The further analysis showed that the PDS area with south facing slope (90° – 270°, clockwise) has better correlation with its corresponding D-part area especially in BT massif. The debris-part area is strongly controlled by SE to W facing PDS slopes for different massifs (for instance: W for LT, SW for KB, SE for KS and SW for BT) which roughly follows the larger coverage of PDS area. The plausible explanation behind this phenomenon could be due to diurnal freeze-thaw cycle, as surface temperature on these slopes varies around the melting point. Local topography (PDS gradient) has strong control over dimension of debris-part especially in BT area but not in western massifs regardless of its latitude.

6. REFERENCES

Ageta, Y., and Higuchi, K. (1984): Estimation of mass balance components of a summer-accumulation type glacier in the Nepal Himalaya. Geografiska Annaler. Series A, Physical Geography, 66(3), 249–255 (doi: 10.2307/520698)

Asahi, K. (1999): Data on inventoried glaciers and its distribution in the eastern part of Nepal Himalaya. Data Report 2 (1994–1998), Cryosphere Research in the Himalaya (CREH). Nagoya, Nagoya University. Institute for Hydrospheric–Atmospheric Sciences; Kathmandu: HM Government of Nepal, Department of Hydrology and Meteorology.

Bajracharya S.R. and 4 others (2014a): Glacier status in Nepal and decadal change from 1980 to 2010 based on Landsat data. Kathmandu: ICIMOD. Pp. 100.

Bajracharya S.R. and 3 others (2014b): The status and decadal change in glaciers in Bhutan from the 1980s to 2010 based on satellite data. Annals of Glaciology 55(66), 159-166, (doi: 10.3189/2014AoG66A125)

Bagla, P. (2009): No sign yet of Himalayan meltdown, Indian report finds, Science, 326, 924–925.

Basnett, S., Kulkarni, A.V. and Bolch, T. (2013): The influence of debris cover and glacial lakes on the recession of glaciers in Sikkim Himalaya, India. Journal of Glaciology, 59(218), 1035–1046 (doi: 10.3189/2013JoG12J184)

Bolch, T., Pieczonka, T. and Benn, D.I. (2011): Multi-decadal mass loss of glaciers in the Everest area (Nepal Himalaya) derived from stereo imagery. Cryosphere, 5, 349–358 (doi: 10.5194/tc-5-349-2011)

Bolch T. and 11 others (2012): The state and fate of Himalayan glaciers. Science, 336, 310–314 (doi:10.1126/science.1215828)

Bolch, T., and 3 others (2008): Planimetric and volumetric glacier changes in the Khumbu Himal, Nepal, since 1962 using Corona, Landsat TM and ASTER data. Journal of Glaciology, 54(187), 592–600 (doi: 10.3189/002214308786570782)

Bookhagen B. and Burbank D.W. (2010): towards a complete Himalayan hydrological budget: The spatiotemporal distribution of snow melt and rainfall and their impact on river discharge. Journal of Geophysical Research, 115(F3), (doi: 10.1029/2009jf001426)

Cogley J.G. and 3 others (2010): Tracking the source of glacier misinformation. Science, 327, 522. (doi:10.1126/science.327.5965.522-a)

Fujita K. and Ageta Y. (2000): Effect of summer accumulation on glacier mass balance on the Tibetan Plateau revealed by mass-balance model. Journal of Glaciology, 46(153). 244–252 (doi: 10.3189/172756500781832945)

Fujita, K., and Sakai, A. (2014): Modelling runoff from a Himalayan debris-covered glacier. Hydrology and Earth System Sciences, 18, 2679–2694 (doi: 10.5194/hess-18-2679-2014)

Gardelle, J. and 3 others (2013): Region-wide glacier mass balances over the Pamir-Karakoram-Himalaya during 1999-2011, The Cryosphere, 7, 1263-1286 (doi: 10.5194/tc-7-1263-2013)

Guo, W. and 10 others (2015): The second Chinese glacier inventory: data, methods and results, Journal of Glaciology, 61, 357–372 (doi: 10.3189/2015JoG14J209, 2015)

Hambrey, M.J. and 5 others (2008): Sedimentological, geomorphological and dynamic context of debris-mantled glaciers, Mount Everest (Sagarmatha) region, Nepal, Quaternary Science Reviews, 27, 2361-2389 (doi: 10.1016/j.quascirev.2008.08.010)

Houze, R.A., Wilton, D.C., and Smull, B.F. (2007): Monsoon convection in the Himalayan region as seen by the TRMM Precipitation Radar, Quarterly Journal of the Royal Meteorological Society, 133, 1389-1411 (doi: 10.1002/qj.106)

Immerzeel W.W., Van Beek LPH, and Bierkens MFP (2010): Climate Change will affect the Asian water towers. Science, 328, 1382–1385 (doi:10.1126/science.1183188)

Kaser G., Groβhauser M. and Marzeion B. (2010): Contribution potential of glaciers to water availability in different climate regimes, P. Natl. Acad. Sci. USA, 107, 20223–20227, (doi: 10, 1073/pnas.1008162107, 2010)

Karma, and 4 others (2003): Glacier distribution in the Himalayas and glacier shrinkage from 1963 to 1993 in the Bhutan Himalayas. Bulletin of Glaciological Research. 20, 29–40

Kulkarni, A.V. and 6 others (2007): Glacial retreat in Himalaya using Indian Remote Sensing satellite data. Current Science, 92(1), 69–74 (doi:10.1117/12.694004)

Kulkarni, A.V., and 3 others (2011): Understanding changes in the Himalayan cryosphere using remote sensing techniques. International Journal of Remote Sensing, 32(3), 601–615 (doi: 10.1080/01431161, 2010.517802)

IPCC (2014): Climate change 2014: Synthesis Report. Contribution of Working Groups I, II and III to the Fifth Assessment Report of the Intergovernmental Panel on Climate Change [Core Writing Team, R.K. Pachauri and L.A. Meyer (eds.)]. IPCC, Geneva, Switzerland, 151 pp.

Luedeling, E., Siebert, S. and Buerkert, A. (2007): Filling the voids in the SRTM elevation model – A TIN-based delta surface approach, International Society of Photogrammetry and Remote Sensing (doi: 10.1016/j.isprs.jprs.2007.05.004)

NSIDC (2016): "All about Glaciers." National Snow and Ice Data Center. Accessed 11th November, 2016 (https://nsidc.org/cryosphere/glaciers)

Nagai, H., Fujita, K., Nuimura, T. and Sakai, A. (2013): Southwest-facing slopes control the formation of debris-covered glaciers in the Bhutan Himalaya. The Cryosphere. 7, 1303–1314, (doi: 10.5194/tc-7-1303-2013)

Nagai, H. and 4 others (2016): Comparison of multiple glacier inventories with a new inventory derived from high-resolution ALOS imagery in the Bhutan Himalaya. The Cryosphere, 10, 65–85 (doi: 10.5194/tc-10-65-2016)

Nie, Y., and 3 others (2010): Glacial change in the vicinity of Mt. Qomolangma (Everest), central high Himalayas since 1976. Journal of Geographical Sciences, 20(5), 667–686 (doi: 10.1007/s11442-010-0803-8)

Nuimura, T. and 12 others (2015): The GAMDAM Glacier Inventory: a quality controlled inventory of Asian glaciers. Cryosphere, 9, 849–864 (doi: 10.5194/tc-9-849-2015)

Paul, F. and 19 others (2013): On the accuracy of glacier outlines derived from remote sensing data, Annals of Glaciology, 54, 171–182 (doi: 10.3189/2013AoG63A296)

Paul, F. and Mölg, N. (2014): Hasty retreat of glaciers in northern Patagonia from 1985 to 2011. Journal of Glaciology, 60(224), 1033–1043 (doi: 10.3189/2014JoG14J104)

Pfeffer, W.T. and 19 others (2014): The Randolph Glacier Inventory a globally complete inventory of glaciers. Journal of Glaciology, 60(221), 537–552 (doi: 10.3189/2014JoG13J176)

Racoviteanu, A.E., and 3 others (2015): Spatial patterns in glacier characteristics and area changes from 1962 to 2006 in the Kanchenjunga-Sikkim area, eastern Himalaya. The Cryosphere, 9, 505–523 (doi: 10.5194/tc-9-505-2015)

Racoviteanu, A.E., and 4 others (2009): Challenges and recommendations in mapping of glacier parameters from space: results of the 2008 Global Land Ice Measurements from Space (GLIMS) workshop, Boulder, Colorado, USA. Annals of Glaciology, 50, 53–69 (DOI: 10.3189/172756410790595804)

Rastner, P., Bolch, T., Mölg, N., Machguth, H., Le, B., and Paul, F. (2012): The first complete inventory of the local glaciers and ice caps on Greenland, The Cryosphere, 6, 1483-1495 (doi:10.5194/tc-6-1483-2012)

Raup, B., and Khalsa, S.J.S. (2010): GLIMS analysis tutorial. Boulder, CO, University of Colorado, National Snow and Ice Data Center, pp–15.

Reuter, H.I., Nelson, A. and Jarvis, A. (2007): An evaluation of void-filling interpolation methods for SRTM data, International Journal of Geographical Information Science, 21, 982–1008 (doi: 10.1080/13658810601169899)

Sakai A. and 5 others (2015): Climate regime of Asian glaciers revealed by GAMDAM Glacier Inventory, The Cryosphere, 9, 865–880 (doi: 10.5194/tc-9-865-2015)

Salerno, F., and 4 others (2008): Glacier surface-area changes in Sagarmatha National Park, Nepal, in the second half of the 20th century, by comparison of historical maps. Journal of Glaciology, 54(187), 738–752 (doi: 10.3189/002214308786570926)

Salerno F. and 10 others (2014): Weak precipitation, warm winters and springs impact glaciers of south slopes of Mt. Everest (Central Himalaya) in the last two decades (1994-2013). The Cryosphere, 9, 1229–1247 (doi: 10.5194/tc-9-1229-2015)

Scherler, D., Bookhagen, B. and Strecker, M.R. (2011a): Spatially variable response of Himalayan glaciers to climate change affected by debris cover, Nature Geoscience, 4, 156–159 (doi: 10.1038/ngeo1068)

Scherler, D., Bookhagen, B. and Strecker, M.R. (2011b): Hillslope-glacier coupling: The interplay of topography and glacial dynamics in High Asia, Journal of Geophysical Research, 116, F02019, (doi: 10.1029/2010JF001751)

Shangguan D. and 10 others (2014): Glacier changes in the Koshi River basin, central Himalaya, from 1976 to 2009, derived from remote-sensing imagery. Annals of Glaciology, 55(56), 61–68 (doi: 10.3189/2014AoG66A057)

Shea J.M. and 4 others (2015): Modelling glacier change in the Everest region, Nepal Himalaya. The Cryosphere, 9, 1105–1128 (doi: 10.5194/tc-9-1105-2015)

Shrestha A.B. and 3 others (2000): Precipitation fluctuations in the Nepal Himalaya and its vicinity and relationship with some large scale climatological parameters. International Journal of Climatology, 20, 317–327 (doi: 10.1002/ (SICI) 1097-0088)

Shrestha, D., Singh, P., and Nakamura, K. (2012) Spatiotemporal variation of rainfall over the central Himalayan region revealed by TRMM Precipitation Radar, Journal of Geophysical Research, 117, D22106, (doi:10.1029/2012JD018140)

Tachikawa T and 12 others (2011): ASTER Global Digital Elevation Model Version 2 – Summary of Validation Results.

Tadono T. and 6 others (2012): Development and validation of new glacial lake inventory in the Bhutan Himalayas using ALOS "Daichi". Global Environmental Research, 16, 31–40.

Thakuri S. and 6 others (2014): Tracing glacier changes since the 1960s on the south slope of Mt. Everest (central Southern Himalaya) using optical satellite imagery., The Cryosphere, 8, 1297–1315 (doi:10.5194/tc-8-1297-2014)

UNEP (2008): Global Glacier Changes: facts and figures. World Glacier Monitoring Service (WGMS), 45 pp.

Wagnon P. and 11 others (2013): Seasonal and annual mass balances of Mera and Pokalde glaciers (Nepal Himalaya) since 2007. The Cryosphere, 7, 1769-1786 (doi: 10.5194/tc-7-1769-2013)

WWF (2005): An Overview of Glaciers, Glacier Retreat, and Subsequent Impacts in Nepal, India and China. 79 pp.

Yamamoto, M.K., Ueno, K., and Nakamura, K. (2011): Comparison of satellite precipitation products with rain gauge data for the Khumbu region, Nepal Himalaya. Journal of the Meteorological Society of Japan, 89(6), 597–610 (doi:10.2151/jmsj.2011-601)

Yao, T. and 15 others (2012): Different glacier status with atmospheric circulations in Tibetan Plateau and surroundings. Nature Climate Change, 2, 663–667 (doi: 10.1038/NCLIMATE1580)

Ye, Q. and 3 others (2006): Monitoring glacier variations on Geladandong Mountain, central Tibetan Plateau, from 1969 to 2002 using remote-sensing and GIS technologies. Journal of Glaciology, 52(179), 537–545 (doi: 10.3189/172756506781828359)

Zemp, M. and 38 others (2015): Historically unprecedented global glacier decline in the early 21st Century, Journal of Glaciology, 61 (228) (doi: 10.3189/2015JoG15J017, 2015)

7. TABLES

Table 1 : Details of the ALOS and Landsat images used for this study. The sensors AP, AA and TM implies ALOS PRISM, ALOS AVNIR-2 and thematic mapper, respectively.

Sensor	ID	Acquisition date
	ALOS	
AP	ALPSMN045823035	4 Dec 2006
	ALPSMN045823040	4 Dec 2006
	ALPSMN045823045	4 Dec 2006
AA	ALAV2A052533040	19 Jan 2007
	ALAV2A052533030	19 Jan 2007
	ALAV2A052533040	19 Jan 2007
AP	ALPSMN094543040	11 Mar 2007
	ALPSMW101983035	24 Dec 2007
	ALPSMW103733040*	05 Jan 2008
	ALPSMB103733095*	05 Jan 2008
	ALPSMW103733035	05 Jan 2008
	ALPSMB104463090*	10 Jan 2008
	ALPSMW104463035*	10 Jan 2008
	ALPSMB104463090*	10 Jan 2008
	ALPSMW104463035*	10 Jan 2008
	ALPSMB105483095*	17 Jan 2008
	ALPSMW105483040*	17 Jan 2008
	ALPSMB105483095*	17 Jan 2008
	ALPSMW105483045*	17 Jan 2008
	ALPSMB103733095*	1 May 2008
	ALPSMW103733040*	1 May 2008
AA	ALAV2A144723030	12 Oct 2008
AP	ALPSMW144723030	12 Oct 2008
	ALPSMW146473040	24 Oct 2008
	ALPSMW148953035	10 Nov 2008

ALPSMW148953040	10 Nov 2008
ALPSMW144723035	10 Dec 2008
ALPSMW153913030	14 Dec 2008
ALPSMB159163100*	19 Jan 2009
ALPSMW159163045	19 Jan 2009
ALPSMB159163100*	19 Jan 2009
ALPSMW159163045*	19 Jan 2009
ALPSMW088563030	18 Feb 2009
ALPSMN097023030	19 Feb 2009
ALPSMN094543035	19 Feb 2009
ALPSMW150703030	20 Feb 2009
ALPSMW148953030	20 Feb 2009
ALPSMW150703035	20 Feb 2009
ALPSMW164123035	22 Feb 2009
ALPSMW071933035	13 May 2009
ALPSMW150703040	25 Aug 2009
ALPSMW153913025	02 Oct 2009
ALPSMB205113090*	30 Nov 2009
ALPSMN205113035*	30 Nov 2009
ALPSMB205113090*	30 Nov 2009
ALPSMN205113035*	30 Nov 2009
ALPSMW146473030	28 Jan 2010
ALPSMW146473035	08 Jan 2010
ALPSMN215323035	08 Feb 2010
ALPSMN215323040	08 Feb 2010
ALPSMN215323045	08 Feb 2010
ALPSMN051073035	03 Feb 2010
ALPSMN104753035	03 Feb 2010
ALPSMN207883040	02 Mar 2010
ALPSMN207883045	03 Mar 2010
ALPSMN219553040	9 Mar 2010

	ALPSMN220283045	14 Mar 2010
	ALPSMB261273080	20 Dec 2010
	ALPSMN261273025	20 Dec 2010
AA	ALAV2A264043040	08 Jan 2011
AP	ALPSMN096293035	14 Jan 2011
	ALPSMN096293040	14 Jan 2011
	ALPSMN096293045	14 Jan 2011
	ALPSMN211383040	09 Feb 2011
	ALPSMN213863030	09 Feb 2011
	ALPSMN213863035	09 Feb 2011
	ALPSMN213863040	10 Feb 2011
	ALPSMN254853045	14 Feb 2011
	ALPSMN260833030	14 Feb 2011
	ALPSMN260833035	14 Feb 2011
	ALPSMN254853040	15 Feb 2011
	ALPSMN259083035	15 Feb 2011
	ALPSMN261563035	31 May 2011
	Landsat	
TM	LT51390411992315ISP00	10 Nov 1992
	LT41400411992266XXX02	22 Sep 1992
	LT51400411992322ISP00	17 Nov 1992
	LT51410401992345ISP00	10 Dec 1992

Table 2 : Details of aerial photographs for the 1992 glacier inventory in the east Nepal Himalaya.

Acquisition month	November 1992
Nominal scale of photographs	1:50,000
Flight altitude	~1000 m from the ground
Photograph coverage	12 km^2 per image
Number of aerial photographs used for editing	
Kanchanjunga region	139
Khumbu region	196
Langtang and Ganesh region	71
Total	406

Table 3 : Glacier statistics in study area. The (±) value given with the glacier area denotes the error calculated, whereas it implies standard deviation for median elevation and slope value. The value in parenthesis depicts the number of glaciers.

Regions	**Langtang**	**Khumbu**	**Kan-Sikkim**	**Bhutan**	**Total**
Glacier area (km^2)	901 ± 149 (704)	1847 ± 291 (1497)	1355 ±208 (1358)	1587 ±243 (1742)	5691 ±893 (5301)
C-type	269 ± 20 (536)	494.6±37.5 (1247)	474.8±35.6 (1157)	614.5±47.6 (1519)	1852.9±140.5 (4459)
D-type	632 ± 129 (168)	1352 ± 254 (250)	880 ± 172 (201)	972 ±196 (223)	3838 ±752 (842)
C-part	448	990	675	752	2867 ± 167
D-part	184	362	204	220	971 ± 236
Median elevation (m a.s.l.)	5513 ± 391	5705 ± 444	5637 ± 392	5531 ± 349	5605 ± 402
C-type	5580 ± 375	5736 ± 453	5654 ± 402	5537 ± 344	5627 ± 404
D-type	5301 ± 369	5542 ± 363	5539 ± 305	5507 ± 385	5484 ± 369
C-part	5463 ± 341	5672 ± 350	5644 ± 280	5611.8 ± 331.6	5608 ± 335.6
D-part	4981 ± 326	5266 ± 345	5246 ± 323	5252 ± 356	5197 ± 358
Slope (degree)	32 ± 8	31 ± 9	30 ± 8	26 ± 7	30 ± 8
C-type	32 ± 9	32 ± 9	31 ± 8	27 ± 7	30 ± 8
D-type	30 ± 7	28 ± 7	27 ± 5	23 ± 5	26 ± 6
C-part	33 ± 7	31 ± 8	30 ± 7	25 ± 6	30 ± 8
D-part	25 ± 9	22 ± 9	21 ± 8	19 ± 6	22 ± 8

8. FIGURES

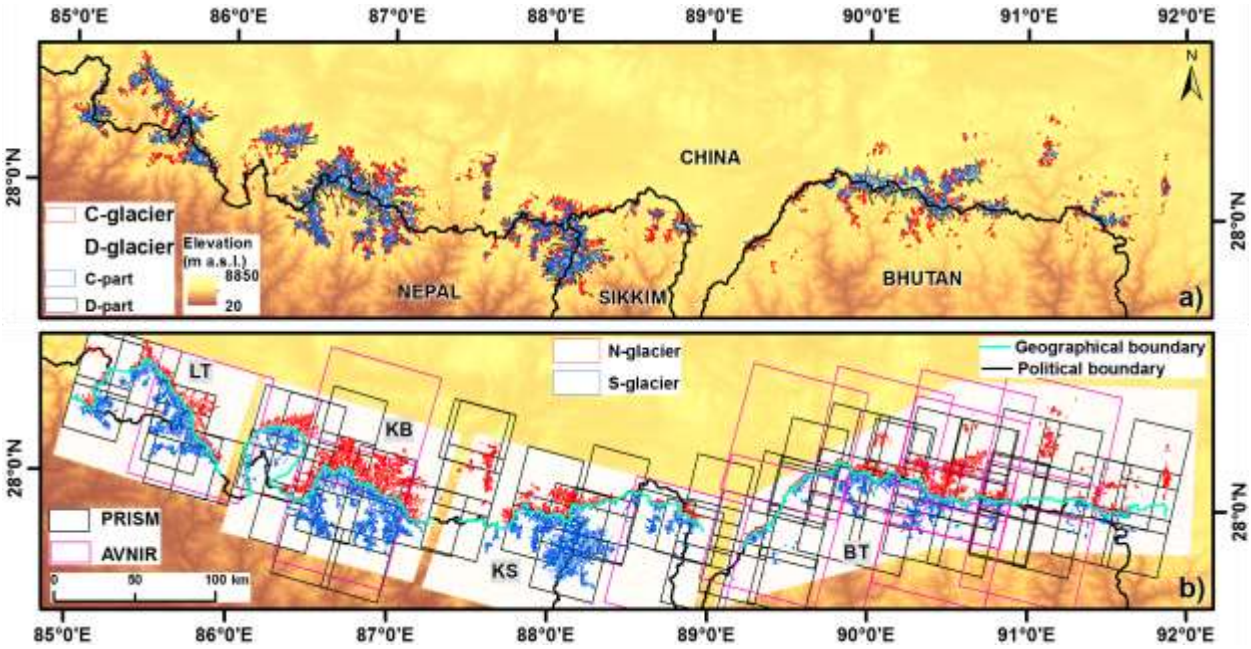

Figure 1 : The spatial extent of (a) glaciers in study area (b) satellite images used for glacier delineation. The D-glacier in further divided into C-part and D-part.

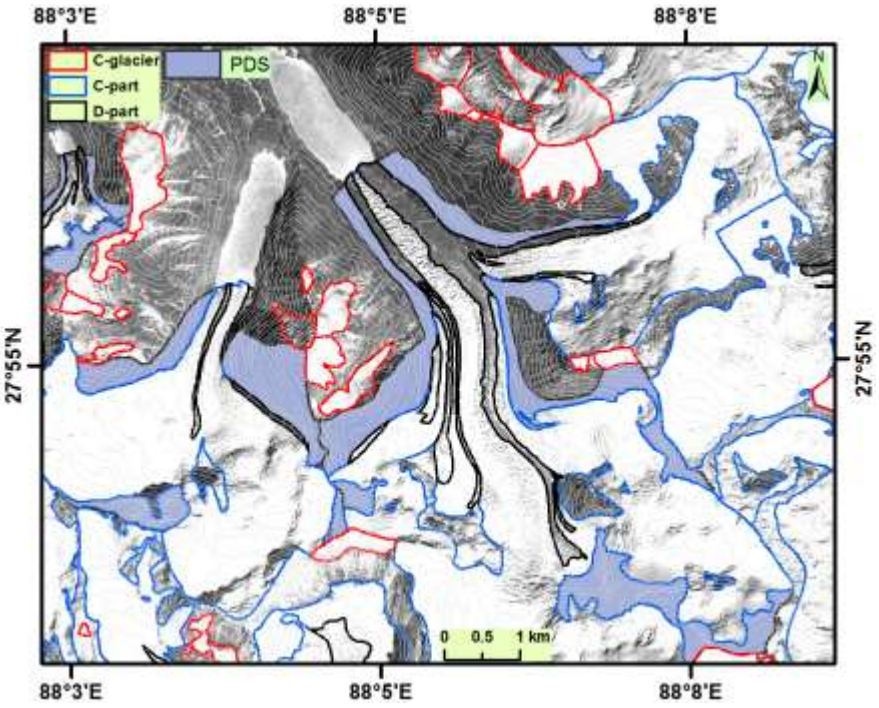

Figure 2 : Example of glacier delineation in KS region where C-glacier, D-glacier, C-part and D-part are depicted. The background image is taken from ALOS PRISM dated 31st October, 2010.

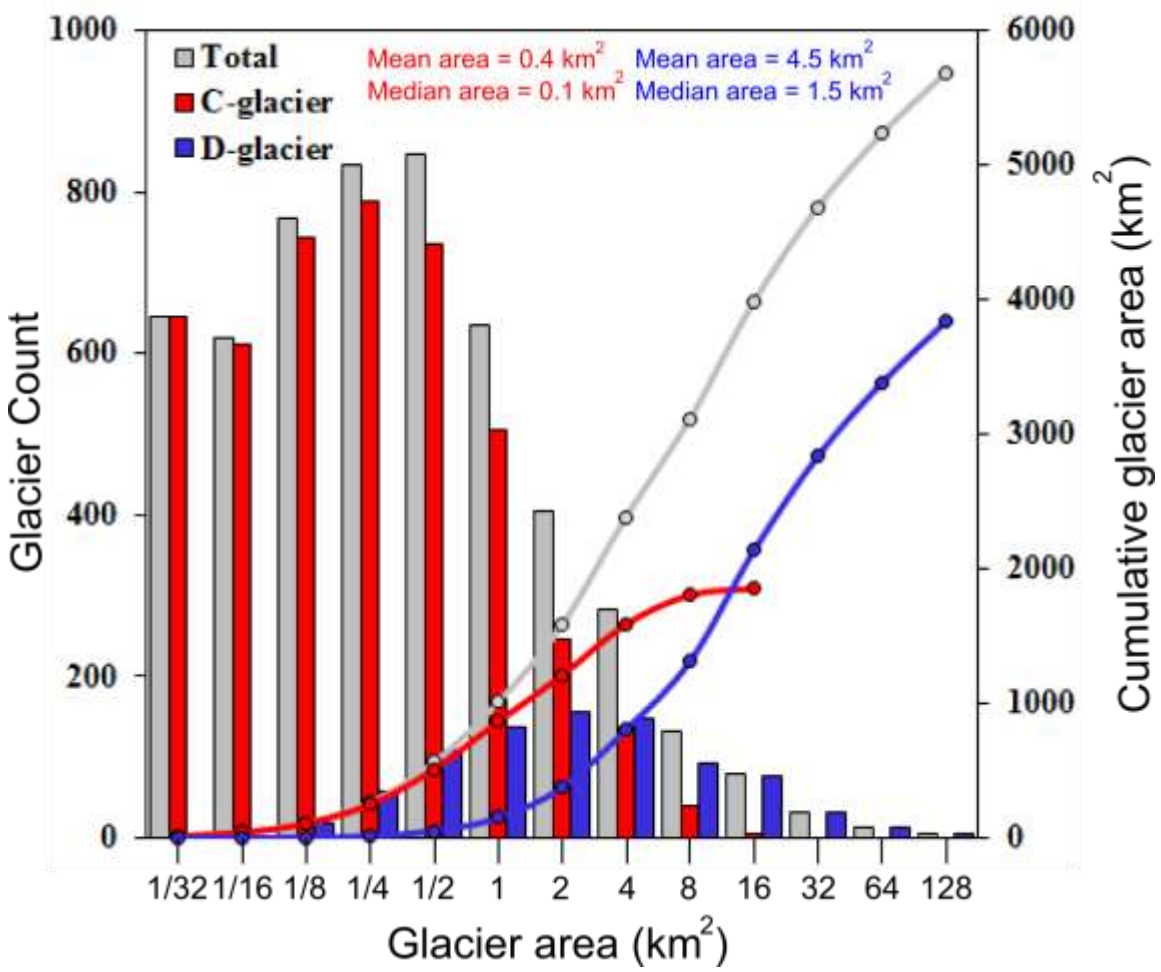

Figure 3 : Histogram of glaciers in study area. The cumulative glacier area in shown in right axis.

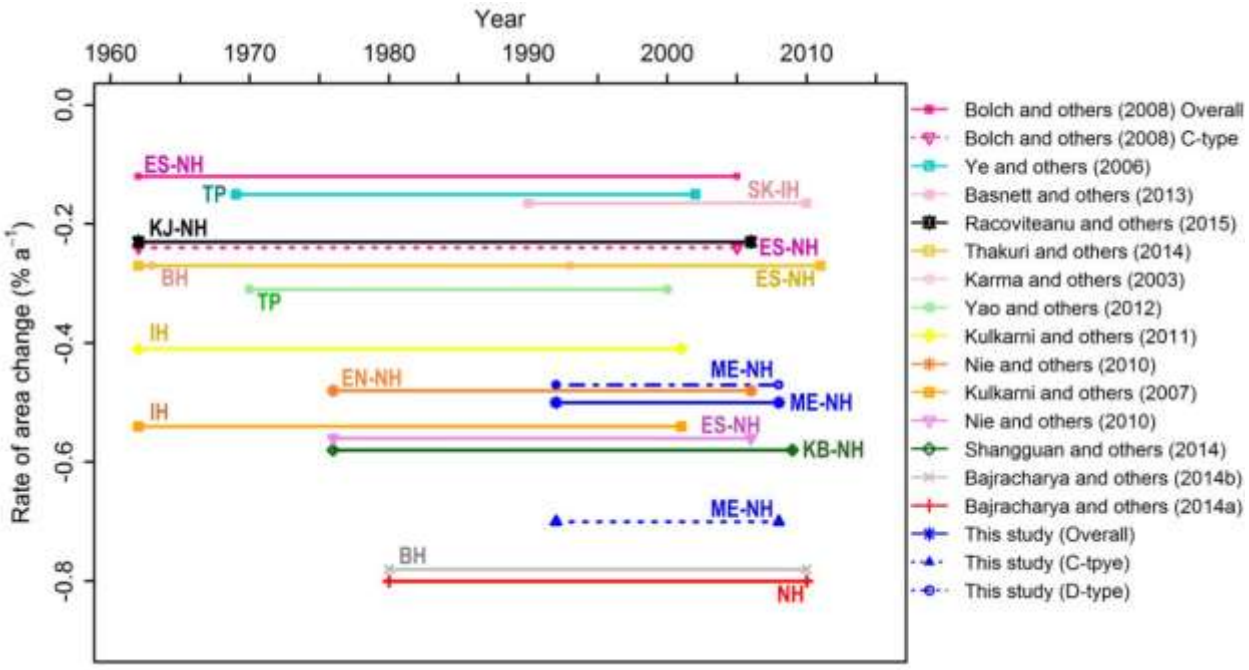

Figure 4 : Comparative study of regional glacier shrinkage over the Himalaya.

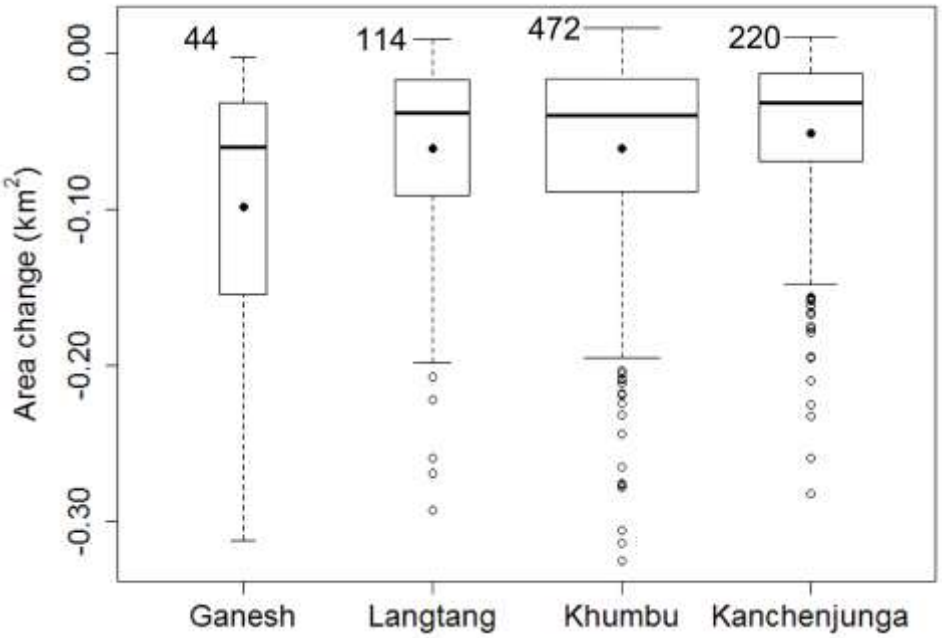

Figure 5 : Intra-regional glaciers shrinkage in study area for last two decades.

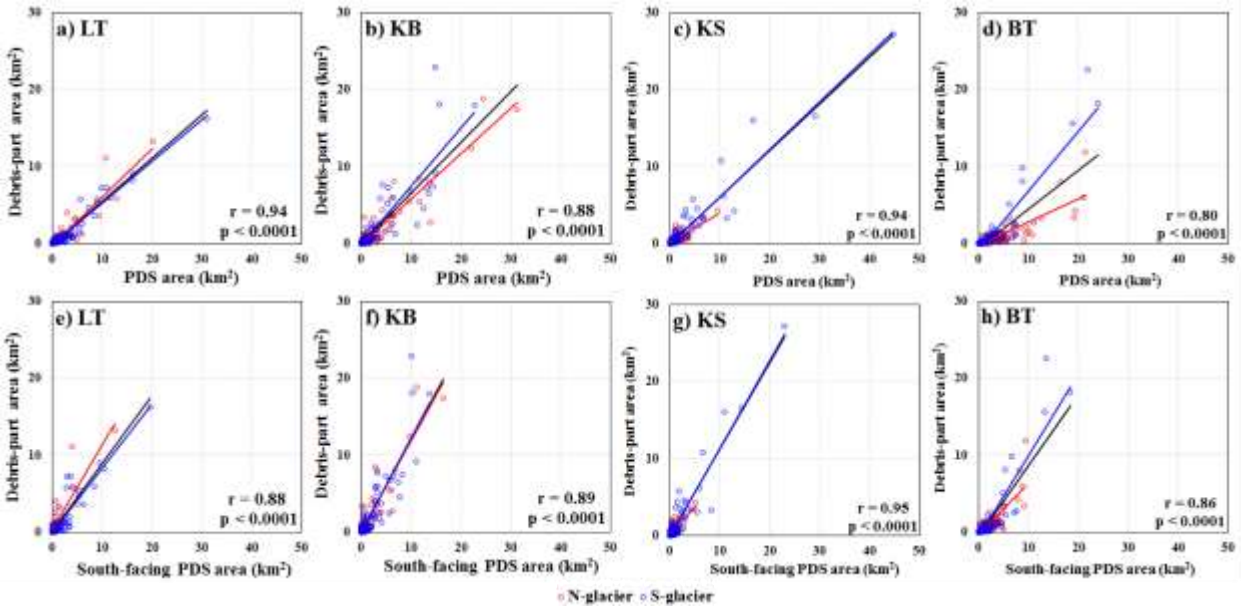

Figure 6 : The relationship between debris-part area and corresponding PDS area (upper panel) and with south-facing (90°–270°, clockwise) PDS area (lower panel).

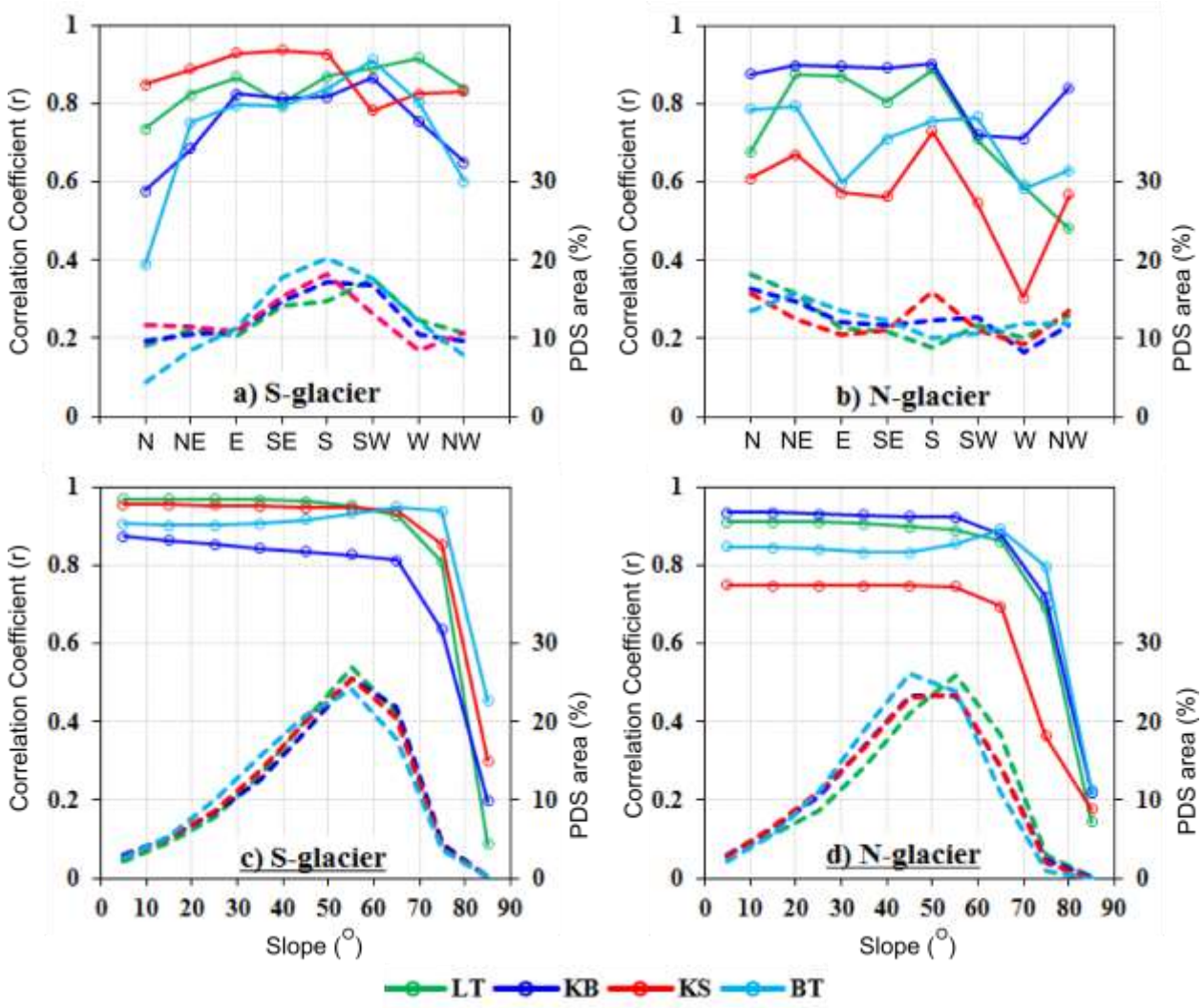

Figure 7 : Correlation coefficient (solid lines) between D-part area and corresponding PDS slope area in different aspects (upper panels), and in different slope ranges (lower panels). The PDS area coverage (%) is shown with dotted lines in right axis.